Beni-Suef University Journal of Basic and Applied Sciences

RESEARCH

Open Access

Tricyclic microwave-assisted synthesis of gold nanoparticles for biomedical applications: combatting multidrug-resistant bacteria and fungus

Sarah Al Azzam[1], Zabih Ullah[2*], Sarfuddin Azmi[1], Mozaffarul Islam[3], Ishtiaque Ahmad[1] and Mohd Kamil Hussain[4]

Abstract

Background Rising global mortality due to antibiotic-resistant pathogens necessitates novel antibacterial and antifungal agents. This study focuses on synthesizing gold nanoparticles (GNPs) via tricyclic microwave irradiation (TMI) to combat Multi-Drug-Resistant Bacteria and Fungus. The demand for sustainable synthesis methods has led to the exploration of TMI for GNP production.

Results Characterization demonstrates consistent, uniform, and dispersed GNPs with trigonal and hexagonal shapes. GNPs sized 20–55 nm exhibit superior antibacterial and antifungal activity, particularly against drug-resistant Gram-positive bacteria. Notably, GNPs display consistent efficacy against drug-resistant fungus and demonstrate potential for broad-spectrum antimicrobial applications.

Conclusion TMI-synthesized GNPs, characterized by their favorable physical properties and size-dependent efficacy, show promise as effective agents against drug-resistant pathogens. Their ability to combat Gram-positive bacteria, Gram-negative bacteria, and drug-resistant fungus positions them as valuable tools in biomedical sciences. By addressing the urgent need for novel antimicrobial agents, TMI-synthesized GNPs offer a sustainable solution to the escalating global health challenge of antibiotic resistance.

Keywords Gold nanoparticles, Reduction synthesis, Drug resistance, Antibacterial, Antifungal

1 Background

Morbidity and mortality resulting from chronic diseases are consequences of bacterial and fungal infections, presenting a significant global health issue and economic burden [1, 2]. The primary approach to combat this global epidemic involves the use of antibiotics. Furthermore, the metabolic byproducts released by humans significantly impact the surrounding environment, contributing to the development of resistance among various microbes. Unfortunately, the continuous release of antibiotics into the environment fosters the development of resistance in microbes initially sensitive to these drugs [3]. Conversely, the natural

*Correspondence:
Zabih Ullah
izabih@gmail.com
[1] Department of Scientific Research Center, Prince Sultan Military Medical City, 11159 Riyadh, Saudi Arabia
[2] Department of Pharmaceutical Sciences, College of Dentistry and Pharmacy, Buraydah Colleges, Al-Qassim, Saudi Arabia
[3] Department of Medical Oncology, Division of Lung Cancer, The Ohio State University, Columbus, OH 43210, USA
[4] Department of Chemistry, Govt. Raza P.G. College, Rampur, U.P. 244901, India

emergence of antibiotic resistance has evolved into a substantial issue, driven by the diminishing effectiveness of existing antimicrobial drugs. This trend is evident in the increasing number of pathogens developing resistance to drug treatments both within hospital settings and in the community as whole. This issue escalated rapidly due to the widespread indiscriminate use of the drugs, which evolved in microorganism strains developing high resistance to the treatments [4–6]. Recently, the U.S. Centers for Disease Control and Prevention reported that antibiotic-resistant microbes are the cause of millions of chronic infections and thousands of death every year [7]. In spite of substantial investments aimed at addressing the notable increase in multidrug-resistant (MDR) bacterial strains, it is disheartening to note that the rate of MDR evolution surpasses the development of advanced classes of antibiotics [8]. In response to the escalating demand for solutions, there is an urgent need to explore innovative and less toxic approaches to prevent and combat multidrug-resistant (MDR) bacterial strains [9]. In contemporary healthcare, nanomedicine has gained widespread popularity as a potent strategy in combating drug-resistant microbes. This approach harnesses the unique properties of nanoscale materials to enhance drug delivery, targeting, and efficacy, offering a promising avenue to overcome challenges posed by microbial resistance in the medical field [10–15].

Recent exploration indicates that nanotechnology holds significant potential in addressing bacterial resistance through the use of nanoparticles. These particles, typically in the size range of 10–100 nm, exhibit unique physical and chemical characteristics. Metal nanoparticles, in particular, showcase exceptional properties attributable to their small size and large surface-to-volume ratio [16, 17]. This enables close interaction with microorganisms, enhancing antibacterial efficacy substantially [11, 18]. Recent reports highlight that the physico-chemical properties of gold nanoparticles (GNPs) create favorable conditions for interaction with microorganisms. This unique property enhances the efficacy of GNPs in suppressing microbial proliferation. Notably, the interaction inhibits DNA/protein synthesis, leading to the death of the microbes. This striking feature underscores the potential of GNPs as effective agents against microbial threats [19–24]. The notable properties of nanoparticles have positioned them as a preferred option in addressing antibiotic resistance. Therefore, nanomedicine, especially metallic nanoparticles like GNPs, emerges as a vital strategy, leveraging unique physico-chemical properties to effectively combat microbial resistance. This approach holds promise in overcoming antibiotic challenges and addressing the urgent need for innovative solutions in the field of medicine.

The sustainable synthesis of nanoparticles employs eco-friendly methods, minimizing the use of hazardous materials and energy consumption. This approach prioritizes biocompatibility, reduces waste generation, and ensures a minimal environmental footprint, making it a promising avenue for environmentally conscious applications in various fields, including biomedicine and catalysis [25–27]. The primary objective of this study is to develop advanced and rapid methods for synthesizing GNPs using minimal chemicals and a commercial microwave. The goal is to produce uniform, dispersed, and size-controlled nanoparticles and assess their efficacy in combating multidrug-resistant bacteria. Current methods either yield unstable, non-uniform nanoparticles or use toxic chemicals, increasing metal toxicity to mammalian cells, environmental pollution, and cost.

The tricyclic microwave irradiation (TMI) method for preparing gold nanoparticles offers rapid, controlled synthesis with uniform size and shape. Microwave heating enables homogeneous energy distribution, enhancing yield and efficiency while allowing versatile reaction conditions adjustment. TMI is energy-efficient and scalable, making it suitable for industrial applications. Compared to green synthesis methods, TMI provides faster synthesis, precise control over nanoparticle properties, and efficient energy utilization, making it a promising approach for advanced nanoparticle fabrication.

The synthesized GNPs have potential biomedical applications, particularly in antimicrobial activity against multidrug-resistant bacteria and fungus.

2 Methods

Chloroauric acid (HAuCl4), citric acid, Cetrimonium bromide (CTAB), 2,7-Dihydroxynaphthalene, hydrazine hydrate, and Sodium citrate were obtained from Sigma-Aldrich (St Louis, MO, USA). Whereas, all the microbes were procured from American Type Culture Collection (ATCC; Manassas, VA, USA).

2.1 Synthesis of nanoparticles

In the first method, for the synthesis of the GNPs, we used approximately 15 ml of 10 mM chloroauric acid (HAuCl4) H_2O, citric acid, and 0.2 mg of cetrimonium bromide (CTAB) [28]. The mixture was continuously stirred to obtain an aqueous solution. This solution was subjected to TMI, i.e., the mixture was heated in a commercial microwave oven at 100 W power for three times ending at 60 s with 20 s intervals. The heating results in an immediate change of color of the solution from light yellow to shining orange, indicating the formation of GNPs. In the second and third methods we used different

reducing agents including Sodium Citrate (50 mL, trisodium citrate, 2.2 mM) with HAuCl4 · 3H2O (1 mL, 10 mM) and hydrazine hydrate (10 ml) with 30 ml of HAuCl4 · 3H2O (10 mM), respectively. These mixtures were stirred separately and subjected to TMI as stated above.

2.2 Characterization of nanoparticles

The GNPs were characterized using various instruments to ensure the uniformity, size, shape, and dispersion of the nanoparticles.

2.3 UV–Vis spectrophotometry

To investigate the changes in surface plasmon resonance (SPR) of the synthesized GNPs Spectrophotometric analysis (Cary 60 UV–Vis, Agilent Technologies, CA, USA) was performed at the spectrum range of 300–800 nm. The procedure was repeated from 24 h to 30 days to measure the stability of the GNPs.

2.4 Scanning electron microscopy

Surface morphology of GNPs was determined using a scanning electron microscope (SEM; EVO LS10; Zeiss, Cambridge, UK). GNP samples were mounted on stubs having adhesive carbon tapes and coated with gold under vacuum conditions with a Q150R sputter coater (Quorum Technologies Ltd. East Sussex, UK). The whole process was carried out in Argon atmosphere at a current of 20 mA and in 120 s. Afterward, the GNPs were examined and photographed to study the surface properties.

2.5 Transmission electron microscope

For TEM analysis, a drop of the GNP suspension from three different formulations was placed on a carbon-coated copper grid which was negatively stained with 2% phosphotungstic acid and left to dry naturally. After drying sample was placed under TEM (JEM-1230; JEOL, Tokyo, Japan) to be examined and photographed.

2.6 Particle size, polydispersity index, and zeta potential

The particle size, zeta potential, and PDI, of the GNPs, were measured by dynamic light scattering principle with the help of Zetasizer (Nano ZS analyzer; Malvern Instruments, Malvern, UK). The colloidal solution containing GNPs was diluted with the help of distilled water and mixed properly. Helium laser was used as a light source, which helps in collecting light scattering data. Photon correlation spectroscopy were applied to obtain the mean results.

2.7 Antibacterial activity

2.7.1 The microbes and growth conditions

The efficacy of GNPs was evaluated against Gram-positive and Gram-negative bacteria and fungus. Gram-positive bacteria include *S. aureus* (ATCC 29213, Vancomycin-resistant), *B. subtilis* (ATCC NCTC10400, sensitive strain), and Methicillin-resistant *staphylococcus aureus (MRSA)* (ATCC 43300), whereas, Gram-negative bacteria include *P. aeruginosa* (ATCC 27853, Multidrug-resistant), *E. coli* (ATCC 25922, Fluoroquinolone resistant), and *E. coli* (ATCC 10536, Vancomycin-resistant). Moreover, fungal species tested was *C. albicans* (ATCC 10231, Fluconazole resistant). Bacterial species were sub-cultured and maintained in tryptic soya broth (TSB) (Oxoid, Ltd., Basingstoke, UK). Additionally, the antifungal efficacy of GNPs was tested by using fluconazole-resistant fungus *Candida albicans*.

2.7.2 Zone inhibition assay

Briefly, in the qualitative assay, bacterial strains were grown at 37 °C with shaking in appropriate growth medium in aerobic condition to the mid-log phase. Subsequently, three different GNPs of one concentration 500 µg (10 µl) from the stock of 50 mg/mL spotted on LB agar plate. As an applied spot of the extract on Petri plate, dried, bacterial cells of the count of approximately 10^7 cells/mL were spread by mixing in melted soft LB agar for even distribution across the Petri plate surface. To see bacterial sensitivity, the zone of inhibition of different type of gold nanoparticle was compared with a standard broad-spectrum conventional antibiotic. For positive and negative controls, a spot of antibiotic (Positive control for bacterial strain used antibiotics-Azithromycin; 2.5 mg/mL and for fungus used fluconazole 2.5 mg/mL) and solvent used to suspend gold nanoparticle was applied on Petri plate.

2.7.3 Broth dilution assay

For quantitative assessment of antibacterial efficacy of gold nanoparticle, broth dilution assay was done in 96-well microtiter plates against different Gram-positive and Gram-negative bacterial strains. In brief, bacterial strains were grown at 37 °C with shaking in appropriate growth medium in aerobic condition to the mid-log phase, determined by the optical density at 600 nm, subsequently diluted in same media to the level of 10^5 CFU/mL. After that, 100 µl of this count was added in 100 µl of water containing twofold serially diluted different gold nanoparticle in each well and incubated for 18–20 h at 37 °C. Gold nanoparticle antibacterial activities were expressed as their minimum inhibitory concentration (MIC) (the exact concentration which resulted in

90–100% inhibition of microbial growth), assessed by measuring the absorbance at 600 nm. For positive and negative control, broad-spectrum antibiotics azithromycin and solvent used for suspending nanoparticle were employed.

2.8 Scanning *electron* microscopy of *bacteria*

The SEM observation of untreated (control) and GNPs treated bacteria was performed as per the earlier published method [29] with little modifications. Bacteria in the exponential growth phase were treated as control. Bacteria of mid long phase diluted to 10^6 CFU/mL and incubated with three-time of MIC of respected type of GNPs for 2 h with mild shaking at 37 °C. Thereafter, treated samples were centrifuged at 2000 rpm for 15 min. Bacterial pellets were washed three times with 10 mM phosphate buffer saline (PBS) and then fixed in acetic acid/ethanol (1:3) for around 20 min at 25 °C. The fixed cells were washed with PBS and re-suspended in Milli-Q Type-1 water for further examination by SEM (SEM; EVO LS10; Zeiss, Cambridge, UK).

2.9 Statistical analysis

The characterization and antibacterial activity of GNPs were performed in triplicates. ANOVA was used for testing between groups, and a p-value of <0.05 was considered as significant. The antibacterial activity data for testing were imported to Statistical Package for the Social Sciences (SPSS) software, version 14.0 (SPSS Inc., Chicago, IL, United States).

3 Results

3.1 Synthesis and characterization of GNPs

GNPs were synthesized by reduction of $HAuCl_4$ using different types of reducing agents, including Citric acid + CTAB, Sodium citrate, and Hydrazine hydrate (Table 1). During the process, the formation of GNPs was established by the appearance of ruby red color. All three formulations were positive for this color change. Furthermore, the formation of nanoparticles was confirmed by measuring the absorbance using a UV spectrophotometer in the range of 300–800 nm (Fig. 1), with maximum absorbance (λmax) peaks at 482, 495, and 506 nm for GNP1, GNP2, and GNP3, respectively. This demonstrates a shifting and broadening of absorption peaks from GNP1 to GNP3, indicative of smaller particle size. TEM images confirmed the formation of GNPs, revealing nanoparticles of trigonal, spherical, tetragonal, hexagonal, and other shapes (Fig. 2). The NPs of GNP1 were larger with irregular contours compared to GNP2, which contained smaller particles with spherical shapes. GNP3 formulation contained even smaller particles than the other formulations. SEM images showed that the nanoparticles have a smooth and multizonal surface, with GNP3 particles being smaller and more spherical compared to the other two formulations (Fig. 3). Particle size, size distribution, and zeta potential were measured using a Zetasizer (Table 2). The data indicated that the use of citric acid + CTAB as reducing agents resulted in the formation of larger nanoparticles (55 ± 6 nm), sodium citrate produced medium-sized GNPs (23 ± 4 nm), and hydrazine hydrate led to the smallest GNPs (9 ± 3 nm). The produced nanoparticles had low PDI values of 0.21 ± 0.05, 0.26 ± 0.06, and 0.16 ± 0.03 for GNP1, GNP2, and GNP3, respectively (Fig. 4). Additionally, all three formulations were found to have a negative zeta potential of −30 ± 2.8, −28 ± 3.2, and −18 ± 2.6, respectively.

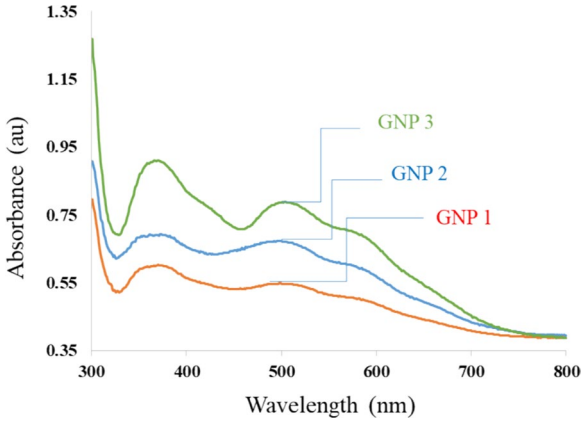

Fig. 1 Characterization of GNPs (GNP1, GNP2 and GNP3) by UV–Visible spectrophotometry. Note: Absorption spectrum showing a shift toward higher wavelength as the particle size decreases. Abbreviations: GNPs, gold nanoparticles

Table 1 Scheme of preparation of nanoparticles with different reducing agents

Nanoparticles	Base	Reducing agents
GNP1	10 mM Chloroauric acid	Citric acid + CTAB
GNP2	10 mM Chloroauric acid	Sodium citrate
GNP3	10 mM Chloroauric acid	Hydrazine hydrate

Citric acid and CTAB were used in combination

GNP gold nanoparticles, *CTAB* cetyltrimethyl-ammonium bromide

3.2 Antibacterial activity

The newly synthesized nanoparticles were subjected to antibacterial efficacy testing using two primary assays: the zone inhibition assay and the broth dilution assay. These tests targeted a range of organisms, including Gram-positive bacteria (*S. aureus, B. subtilis, MRSA*), Gram-negative bacteria (*E. coli, P. aeruginosa*), and the fungus *C. albicans*.

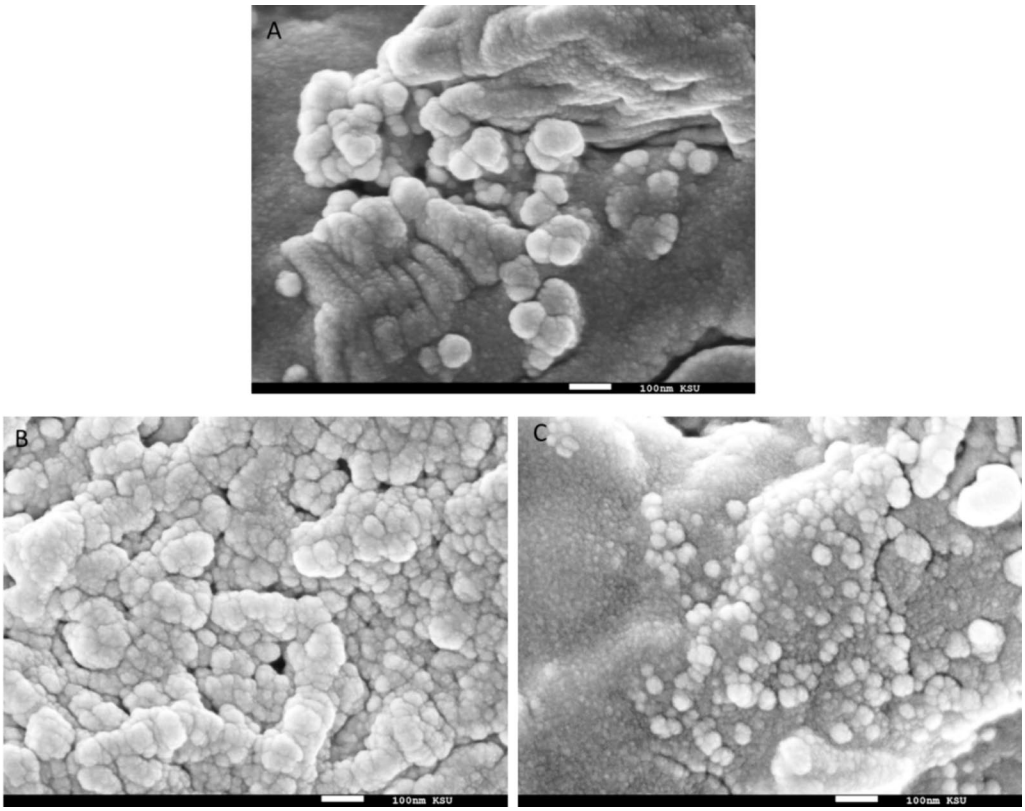

Fig. 2 SEM micrograph of GNPs formulation for GNP1 (**A**), GNP2 (**B**) and GNP3 (**C**). Note: As shown in the figure, the newly synthesized GNPs when observed under SEM were found to have a multigonal bright surface. Abbreviations: SEM, scanning electron microscope, GNPs, gold nanoparticles

3.2.1 Zone inhibition assay

In the qualitative assay, we observed a significant zone of inhibition for each type of nanoparticle against different Gram-positive and Gram-negative bacterial strains and fungus compared to the positive control (Fig. 5). Zone of inhibition in the bacteria including *S. aureus, B. subtilis,* and *MRSA* was found in all three-nanoparticle formulations. Whereas maximum zone of inhibition was observed in the case of Gram-negative bacteria including *E. coli* and *P. aeruginosa*. GNPs were found to be equally effective for fungus *C. albicans* as well. In all the developed formulations, the GNP1 was found to be having a maximum zone of inhibition except in the case of *E. coli*, where maximum efficacy was shown by the GNP2. *C. albicans* was found to be equally sensitive for all the GNPs, whereas, maximum efficacy was reported to be with GNP1followed by GNP2 and GNP3. Although, in the zone inhibition assay, we used a significantly high concentration of gold nanoparticle. Therefore, in order to evaluate the value of the antibacterial activity quantitatively, we performed broth dilution assay.

3.2.2 Broth dilution assay

In this assay, we notice that GNP1 and GNP2 were approximately twofold more active compared to GNP3 ($p < 0.05$) and simultaneously we observed that Gram-positive strains were more sensitive than Gram-negative strains against each type of nanoparticles (Table 3). GNP1 was found to be more effective against *B. subtilis* and *S. aureus* with a MIC level of 21.48 ± 2.24 and 23.62 ± 3.23 µg/mL, respectively. Whereas, GNP3 was found to be lesser effective for *B. subtilis* and *S. aureus* with a MIC level of 44.58 ± 5.32 and 51.65 ± 5.47 µg/mL, respectively. *E. coli* and *P. aeruginosa* were found to be comparatively less sensitive with the GNPs with a MIC range of 41–43 µg/mL for GNP1 and GNP2. Whereas, the MIC level was doubled for *E. coli,* and *P. aeruginosa* in case of GNP3 which we observed as 98.24 ± 6.95 and 102.48 ± 7.59 µg/mL, respectively ($p < 0.05$). Similar to bacteria, the fungus *C. albicans* was more susceptible to the GNP1 in comparison to other preparations. The GNP1 was having a MIC of 32.65 ± 3.26 µg/mL for *C. albicans*, whereas, GNP3 exhibited relatively lesser MIC of 53.84 ± 4.62 µg/mL for *C. albicans* ($p < 0.05$). The

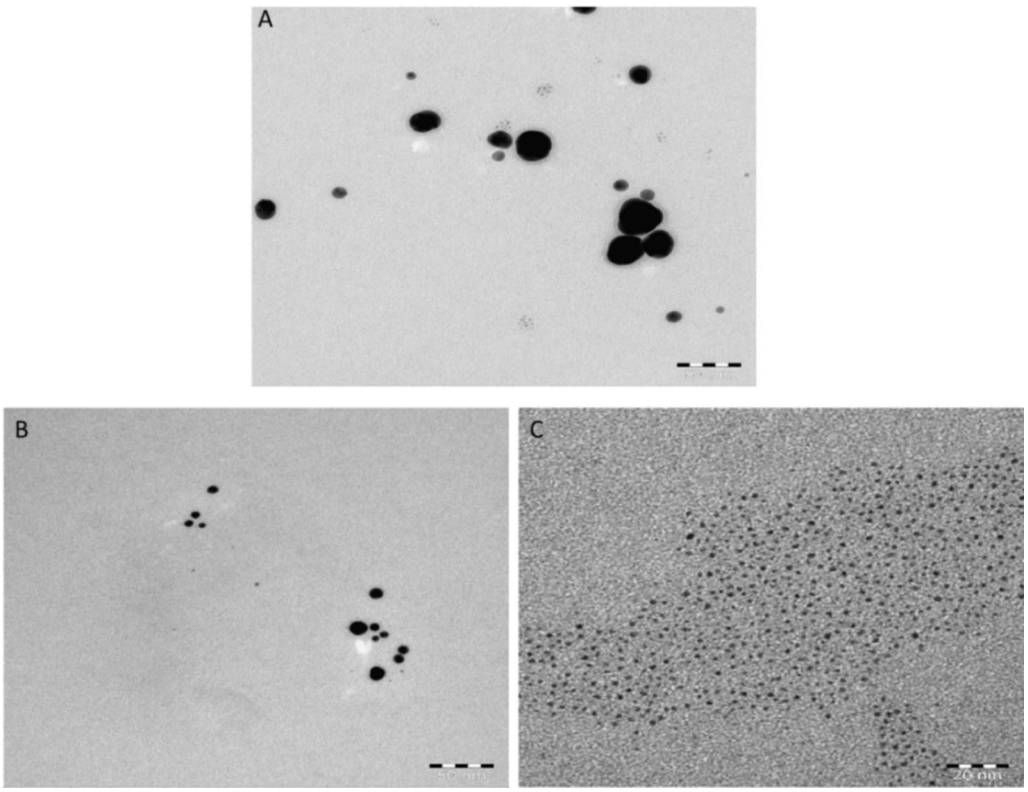

Fig. 3 TEM photographs of GNPs formulation for GNP1 (**A**), GNP2 (**B**) and GNP3 (**C**). Notes: TEM photographs demonstrate that the prepared nanoparticles are trigonal, spherical and hexagonal in shapes, Scale bar = 50 nm. Abbreviations: TEM, transmission electron microscope, GNPs, gold nanoparticles

Table 2 Characterization of GNPs by DLS using Zetasizer

Nanoparticles	Particle size (nm)	PDI	Zeta potential (mV)
GNP1	55 ± 6	0.21 ± 0.05	−30 ± 2.8
GNP2	23 ± 4	0.26 ± 0.06	−28 ± 3.2
GNP3	9 ± 3	0.16 ± 0.03	−18 ± 2.6

Mean ± SD (n = 3) for three formulations

GNP gold nanoparticles, *PDI* polydispersity index, *DLS* dynamic light scattering, *SD* standard deviation

antibacterial efficacy of all three GNPs is summarized in Table 3.

It is evident from the data that all the formulations were active against the drug-resistant bacteria and fungus, but the intensity of activity was found to be different for each preparation. This may be due to the different sizes of the nanoparticles. The formulations having a particle size in the range of 20–50 nm (GNP1 and GNP2) are having better antibacterial and antifungal efficacy as compared with GNP3. The GNPs whose size was < 20 nm (GNP3) has been demonstrated lesser activity against these pathogens.

4 Discussion

The choice of different reducing agents in this study aimed to explore the formation of ideal nanoparticles through a common synthesis technique. The use of TMI resulted in the quick formation of nanoparticles, which is advantageous over traditional methods that require several hours of incubation to produce nanoparticles. The varying absorption peaks observed in the UV–Vis spectrums indicate differences in particle size among the formulations, corroborated by TEM and SEM imaging. The difference in particle size and shape among the formulations is attributed to the use of different reducing agents. This variability highlights the importance of selecting appropriate reducing agents based on desired nanoparticle characteristics. The observed smooth and multizonal surface of the GNPs, as well as the size and shape variations, demonstrate the versatility of the synthesis process. The measured zeta potential values indicate that all three nanoparticle formulations possess a stable negative charge, contributing to their stability in suspension. The low polydispersity index (PDI) across all formulations suggests uniformity in particle size, which is crucial for many biomedical applications. Our findings suggest that

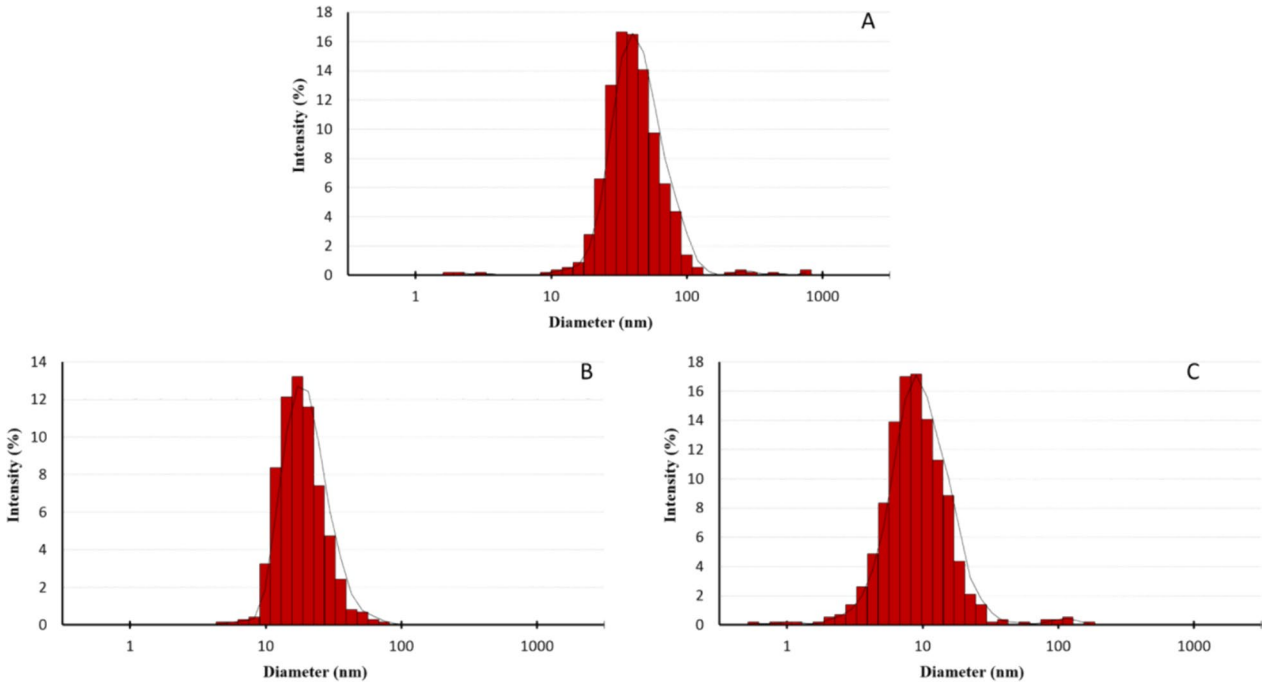

Fig. 4 DLS histograms GNPs formulation for GNP1 (**A**), GNP2 (**B**) and GNP3 (**C**). Notes: Figure demonstrate the size distribution of GNPs. Illustrative histograms from DLS data for diameter. Abbreviations: DLS, dynamic light scattering GNPs, gold nanoparticles

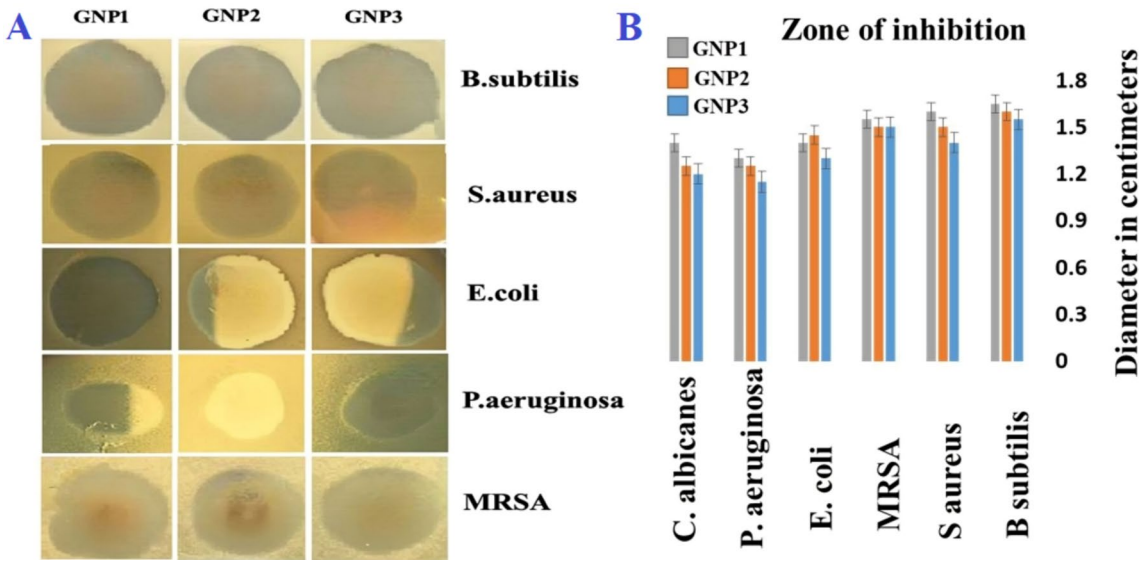

Fig. 5 Zone of inhibition of different bacteria and after treatment after treatment with GNPs (**A**). Zone inhibition diameters (cm) exerted by corresponding formulations GNP1, GNP2 and GNP3 (**B**). Abbreviations: GNPs, gold nanoparticles, MRSA, Methicillin-resistant *Staphylococcus aureus*

the synthesis of GNPs can be effectively tailored through the choice of reducing agents, offering rapid and straightforward methods to produce size-controlled GNPs. This contrasts with conventional synthesis methods, which are often expensive, complicated, time-consuming, and result in unstable nanoparticles. The produced GNPs hold potential for various biomedical applications,

Table 3 MICs level of different microbes after treatment with developed nanoparticles formulations

Microbes	MICs (µg/mL)*		
	GNP1	GNP2	GNP3
S. aureus	23.62 ± 3.23	24.53 ± 3.54	51.65 ± 5.47
B. subtilis	21.48 ± 2.24	25.36 ± 3.42	44.58 ± 5.32
C. albicans	32.65 ± 3.26	31.46 ± 4.58	53.84 ± 4.62
E. coli	41.46 ± 2.57	42.58 ± 5.63	98.24 ± 6.95
P. aeruginosa	52.63 ± 5.64	46.57 ± 4.51	102.48 ± 7.59
MRSA	32.58 ± 5.43	29.54 ± 3.47	63.53 ± 6.85

* All MICs values against all bacterium are Mean ± SD (n = 3)

GNP gold nanoparticles, *MICs* minimum inhibitory concentrations

underscoring the importance of optimizing synthesis techniques to meet specific demands.

Our research findings are consistent with a previous study that examined the antimicrobial effects of silver and gold nanoparticles (NPs) and the resistance developed by S. aureus. It was reported that gold nanoparticles (GNPs) with an average size of 20 nm demonstrated a lower minimum inhibitory concentration (MIC) compared to GNPs with an average particle size of 10 nm [18]. In another study, it was found that smaller gold nanoparticles (GNPs) were more effective in killing bacteria compared to larger GNPs. However, the formulations in the study encompassed a wide size range of GNPs, ranging from 6 to 34 nm for the first formulation and 20 to 40 nm for the second formulation. This wide range of sizes complicates the interpretation of results, making it difficult to draw definitive conclusions [30]. The properties and application of metal nanoparticles are strongly dependent on their size and shape [31]. For therapeutic applications, gold in nanoparticle form is much more efficacious than in a macroscale form. During the manufacturing process, certain parameters determine the size of the final product. For example, smaller nanoparticles are obtained under conditions of fast reaction rates and more significant amounts of the stabilizing agent [32]. Higher temperatures also result in more monodispersed particles [33].

In our study, we also found that the antimicrobial activity of GNPs are different in Gram-positive and Gram-negative bacteria. The GNPs prepared by all three methods are having higher activity toward Gram-positive than Gram-negative bacteria. This may be due to the difference in the composition and structure of the cell wall membrane of microbes. Plausibly, composition of bacterial cell wall play crucial role in imparting differential antibacterial property to GNPs. This phenomenon can be explained in terms of zeta potential and lipopolysaccharide composition of the cell wall. Gram-negative bacteria are having little higher negative zeta potential due to the presence of lipopolysaccharides; a component of the cell wall. Whereas, Gram-positive bacteria are having lower level of negative zeta potential due to the absence of lipopolysaccharides, which is probably one of the reason of higher activity of GNPs against Gram-positive bacteria [34]. Additionally, as mentioned in the methodology, we performed SEM analysis of control as well as different GNPs treated bacteria (Fig. 6). It can be seen clearly from the images that the bacteria in the control group showed undetectable morphological changes. However, the other treatment groups like GNP1, GNP2, and GNP3 exhibited remarkable damage to the bacterial cell wall. Hence, it can be concluded that the GNPs are having potential to penetrate the cell wall of bacteria and can make it dysfunctional. Because of this extraordinary cell penetration property, GNPs are having great potential and can be utilized in the treatment of various infectious diseases caused by drug-resistant microbes. Furthermore, gold can be used in various fields of medicine and biotechnology, making it one of the most essential elements as a nanoscale material. One of the main reasons why incorporating GNPs into many applications has gained popularity is due to its freeness of toxic heavy metals and reactive chemical functional groups [35].

GNPs are also being considered as a novel material for labeling, imaging, and assaying applications due to its high absorption and emission of near infrared light that prevents interference from biological molecules, unlike fluorescence labels [36]. Furthermore, studies about creating metallic and bimetallic nanoparticles in nanoscience have emerged recently due to their attractive properties like optical, electrical, and catalytic possessions. This is enhanced by their large surface area to volume ratios. Nanoparticles of gold and silver usually require stabilizing agents like polyvinylpyrrolidone for their synthesis [37], However, in our research, we opted for microwave-mediated synthesis, which produced stable and efficient GNPs. It offers an excellent alternative to the preparation of metallic nanoparticles in the aqueous solution. The existence of microbial organisms that have drug resistance is the reason why there has been development in the usage of nanoparticles [28].

5 Conclusion

In the present study, we demonstrated TMI mediated synthesis of stable GNPs by using three different reducing agents. These GNPs were characterized for shape and surface morphology and tested for antibacterial and antifungal efficacy using drug-resistant Gram-positive, Gram-negative bacteria, and *C. albicans,*

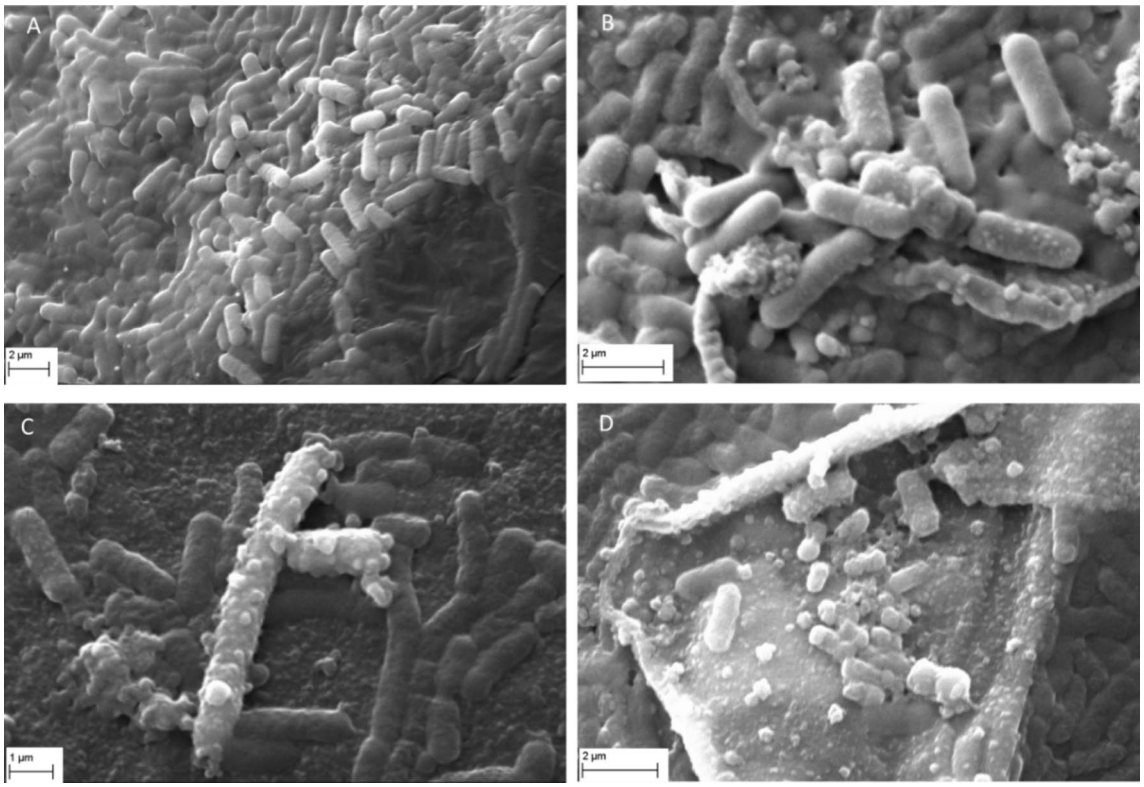

Fig. 6 SEM images of *E. coli* after treatment with GNPs formulations, control (**A**), GNP1 (**B**) GNP2 (**C**) and GNP3 (**D**) demonstrating that the treatment with GNPs causes significant cell damage to the bacteria. Abbreviations: GNPs, gold nanoparticles, SEM, scanning electron microscope

respectively. The prepared nanoparticles were mostly trigonal, spherical and hexagonal in shape with low PDI as an indicator of homogenous dispersion. The intensity of activity of GNPs was found to be size-dependent. The GNPs of size 20–50 nm demonstrated high antibacterial, antifungal activity compared to those with a size of < 20 nm. The nanoparticles showed enhanced activity against Gram-positive than Gram-negative bacteria. The MIC level for GNP1 in case of *B. subtilis* and *S. aureus* was found to be 21.48 ± 2.24 and 23.62 ± 3.23 µg/mL, respectively. Contrastingly, in case of GNP3, we observed significantly higher MIC level (44.58 ± 5.32 and 51.65 ± 5.47 µg/mL) against *B. subtilis* and *S. aureus*. Furthermore, we have noticed that *E. coli* and *P. aeruginosa* showed comparatively lesser sensitivity against all three GNPs, with a MIC range of 41–43 µg/mL for GNP1 and GNP2 and around 100 µg/mL for GNP3. Similarly, against fungal strain *C. albicans,* GNP1 and GNP2 exhibited comparatively much better activity than GNP3. Based on these findings, it can be concluded that the GNPs prepared through TMI technique with Citric acid combine with CTAB and sodium citrate as reducing agents could become a useful tool in eradicating drug-resistant bacteria and fungus. However, the safety of nanoparticles is a matter of concern, and further studies are warranted to identify any toxicological issues associated with these nanomaterials.

Abbreviations

ANOVA	Analysis of Variance
B. subtilis	*Bacillus subtilis*
C. albicans	*Candida albicans*
CDC	Centers for Disease Control and Prevention
CFU/mL	Colony Forming Units per Milliliter
CTAB	Cetyltrimethylammonium Bromide
E. coli	*Escherichia coli*
MIC	Minimum Inhibitory Concentration
MRSA	Methicillin-resistant *Staphylococcus aureus*
NCTC	National Collection of Type Cultures
PBS	Phosphate Buffer Saline
PDI	Polydispersity Index
P. aeruginosa	*Pseudomonas aeruginosa*
SEM	Scanning Electron Microscopy
SEM	Standard Error of the Mean
SPSS	Statistical Package for the Social Sciences
S. aureus	*Staphylococcus aureus*
TMI	Tricyclic Microwave Irradiation
TEM	Transmission Electron Microscopy

Acknowledgements
The authors are grateful to King Abdullah Nanotechnology Center, Riyadh and TEM Lab, Research Center, Faculty of Science, King Saud University Riyadh for their support in morphological characterization of nanoparticles.

Author contributions
1-SAA (Conducted experiments, Analyzed data).) 2- ZU (Designed study, manuscript writing) 3- SA (Analyzed data, manuscript writing), 4-MI (Analyzed data, manuscript writing), 5-IA (manuscript writing), 6-MKH (Analyzed data, manuscript writing). We confirm that the manuscript has been read and approved for submission by all the authors.

Funding
Not applicable.

Availability of data and materials
Not applicable.

Declarations

Ethics approval and consent to participate
Not applicable.

Consent for publication
Not applicable.

Competing interests
The authors declare no conflicts of interest, including financial interests, about the subject matter discussed in this study.

Received: 25 February 2024 Accepted: 1 June 2024
Published online: 07 June 2024

References

1. Ahamad S, Branch S, Harrelson S et al (2021) Primed for global coronavirus pandemic: emerging research and clinical outcome. Eur J Med Chem 209:112862. https://doi.org/10.1016/j.ejmech.2020.112862
2. Hussain MK, Ahmed S, Khan A et al (2023) Mucormycosis: a hidden mystery of fungal infection, possible diagnosis, treatment and development of new therapeutic agents. Eur J Med Chem 246:115010. https://doi.org/10.1016/j.ejmech.2022.115010
3. Pezzi L, Pane A, Annesi F et al (2019) Antimicrobial effects of chemically functionalized and/or photo-heated nanoparticles. Materials (Basel) 12:1078. https://doi.org/10.3390/ma12071078
4. Fasugba O, Das A, Mnatzaganian G et al (2019) Incidence of single-drug resistant, multidrug-resistant and extensively drug-resistant Escherichia coli urinary tract infections: an Australian laboratory-based retrospective study. J Glob Antimicrob Resist 16:254–259. https://doi.org/10.1016/j.jgar.2018.10.026
5. Ding D, Wang B, Zhang X et al (2023) The spread of antibiotic resistance to humans and potential protection strategies. Ecotoxicol Environ Saf 254:114734. https://doi.org/10.1016/j.ecoenv.2023.114734
6. Bobate S, Mahalle S, Dafale NA, Bajaj A (2023) Emergence of environmental antibiotic resistance: mechanism, monitoring and management. Environ Adv 13:100409. https://doi.org/10.1016/j.envadv.2023.100409
7. Antibiotic resistance threats in the United States, 2019. Atlanta, Georgia
8. Cassini A, Högberg LD, Plachouras D et al (2019) Attributable deaths and disability-adjusted life-years caused by infections with antibiotic-resistant bacteria in the EU and the European Economic Area in 2015: a population-level modelling analysis. Lancet Infect Dis 19:56–66. https://doi.org/10.1016/S1473-3099(18)30605-4
9. Awad A, Pampiglione T, Ullah Z (2019) Abdominal tuberculosis with a Pseudo-Sister Mary Joseph nodule mimicking peritoneal carcinomatosis. BMJ Case Rep 12:e229624. https://doi.org/10.1136/bcr-2019-229624
10. Hetta HF, Ramadan YN, Al-Harbi AI et al (2023) Nanotechnology as a promising approach to combat multidrug resistant bacteria: A comprehensive review and future perspectives. Biomedicines 11:413. https://doi.org/10.3390/biomedicines11020413
11. Rubey KM, Brenner JS (2021) Nanomedicine to fight infectious disease. Adv Drug Deliv Rev 179:113996. https://doi.org/10.1016/j.addr.2021.113996
12. Akturk O, Gun Gok Z, Erdemli O, Yigitoglu M (2019) One-pot facile synthesis of silk sericin-capped gold nanoparticles by UVC radiation: Investigation of stability, biocompatibility, and antibacterial activity. J Biomed Mater Res Part A 107:2667–2679. https://doi.org/10.1002/jbm.a.36771
13. Cheng H, Li Y, Huo K et al (2014) Long-lasting in vivo and in vitro antibacterial ability of nanostructured titania coating incorporated with silver nanoparticles. J Biomed Mater Res Part A 102:3488–3499. https://doi.org/10.1002/jbm.a.35019
14. Okada M, Yasuda S, Kimura T et al (2006) Optimization of amino group density on surfaces of titanium dioxide nanoparticles covalently bonded to a silicone substrate for antibacterial and cell adhesion activities. J Biomed Mater Res Part A 76A:95–101. https://doi.org/10.1002/jbm.a.30513
15. Ueda T, Ueda K, Ito K et al (2019) Visible-light-responsive antibacterial activity of Au-incorporated TiO_2 layers formed on Ti–(0–10) at% Au alloys by air oxidation. J Biomed Mater Res Part A 107:991–1000. https://doi.org/10.1002/jbm.a.36624
16. Vaid P, Raizada P, Saini AK, Saini RV (2020) Biogenic silver, gold and copper nanoparticles: a sustainable green chemistry approach for cancer therapy. Sustain Chem Pharm 16:100247. https://doi.org/10.1016/j.scp.2020.100247
17. Rizki IN, Klaypradit W, Patmawati, (2023) Utilization of marine organisms for the green synthesis of silver and gold nanoparticles and their applications: a review. Sustain Chem Pharm 31:100888. https://doi.org/10.1016/j.scp.2022.100888
18. Elbehiry A, Al-Dubaib M, Marzouk E, Moussa I (2019) Antibacterial effects and resistance induction of silver and gold nanoparticles against Staphylococcus aureus -induced mastitis and the potential toxicity in rats. Microbiologyopen 8. https://doi.org/10.1002/mbo3.698
19. Lomelí-Marroquín D, Medina Cruz D, Nieto-Argüello A et al (2019) Starch-mediated synthesis of mono- and bimetallic silver/gold nanoparticles as antimicrobial and anticancer agents. Int J Nanomed 14:2171–2190. https://doi.org/10.2147/IJN.S192757
20. Li J, Tian B, Li T et al (2018) Biosynthesis of Au, Ag and Au–Ag bimetallic nanoparticles using protein extracts of Deinococcus radiodurans and evaluation of their cytotoxicity. Int J Nanomed 13:1411–1424. https://doi.org/10.2147/IJN.S149079
21. Abdel-Kareem MM, Zohri AA (2018) Extracellular mycosynthesis of gold nanoparticles using Trichoderma hamatum: optimization, characterization and antimicrobial activity. Lett Appl Microbiol 67:465–475. https://doi.org/10.1111/lam.13055
22. Tao C (2018) Antimicrobial activity and toxicity of gold nanoparticles: research progress, challenges and prospects. Lett Appl Microbiol 67:537–543. https://doi.org/10.1111/lam.13082
23. Vijayan R, Joseph S, Mathew B (2018) Eco-friendly synthesis of silver and gold nanoparticles with enhanced antimicrobial, antioxidant, and catalytic activities. IET Nanobiotechnol 12:850–856. https://doi.org/10.1049/iet-nbt.2017.0311
24. Hu X, Ahmeda A, Zangeneh MM (2020) Chemical characterization and evaluation of antimicrobial and cutaneous wound healing potentials of gold nanoparticles using Allium saralicum R.M. Fritsch. Appl Organomet Chem 34. https://doi.org/10.1002/aoc.5484
25. Ashraf H, Anjum T, Riaz S et al (2022) Sustainable synthesis of microwave-assisted IONPs using *Spinacia oleracea* L. for control of fungal wilt by modulating the defense system in tomato plants. J Nanobiotechnol 20:8. https://doi.org/10.1186/s12951-021-01204-9
26. Prakash M, Kavitha HP, Abinaya S et al (2022) Green synthesis of bismuth based nanoparticles and its applications: a review. Sustain Chem Pharm 25:100547. https://doi.org/10.1016/j.scp.2021.100547
27. Abdullah JAA, Salah Eddine L, Abderrhmane B et al (2020) Green synthesis and characterization of iron oxide nanoparticles by pheonix dactylifera leaf extract and evaluation of their antioxidant activity. Sustain Chem Pharm 17:100280. https://doi.org/10.1016/j.scp.2020.100280
28. Arshi N, Ahmed F, Kumar S et al (2011) Microwave assisted synthesis of gold nanoparticles and their antibacterial activity against *Escherichia coli*

(*E. coli*). Curr Appl Phys 11:S360–S363. https://doi.org/10.1016/j.cap.2010.11.102
29. Dosunmu E, Chaudhari A, Shree S et al (2015) Silver-coated carbon nanotubes downregulate the expression of Pseudomonas aeruginosa virulence genes: a potential mechanism for their antimicrobial effect. Int J Nanomedicine. https://doi.org/10.2147/IJN.S85219
30. Shamaila S, Zafar N, Riaz S et al (2016) Gold nanoparticles: an efficient antimicrobial agent against enteric bacterial human pathogen. Nanomaterials 6:71. https://doi.org/10.3390/nano6040071
31. Zhang X-D, Wu D, Shen X et al (2011) Size-dependent in vivo toxicity of PEG-coated gold nanoparticles. Int J Nanomed 20:71. https://doi.org/10.2147/IJN.S21657
32. Boussoufi F, Navarro Gallón S, Chang R, Webster T (2018) Synthesis and study of cell-penetrating peptide-modified gold nanoparticles. Int J Nanomed 13:6199–6205. https://doi.org/10.2147/IJN.S168720
33. Zou J, Dai Q, Guda R, et al (2008) Controlled chemical functionalization of gold nanoparticles, pp 31–40
34. Arakha M, Saleem M, Mallick BC, Jha S (2015) The effects of interfacial potential on antimicrobial propensity of ZnO nanoparticle. Sci Rep 5:9578. https://doi.org/10.1038/srep09578
35. Byrne H, Mukherjee S, Naha P (2018) Nano-bio interactions: nanomedicine and nanotoxicology. Int J Environ Res Public Health 15:1222. https://doi.org/10.3390/ijerph15061222
36. Kim S-E, Lee B-R, Lee H et al (2017) Near-infrared plasmonic assemblies of gold nanoparticles with multimodal function for targeted cancer theragnosis. Sci Rep 7:17327. https://doi.org/10.1038/s41598-017-17714-2
37. Pal A, Shah S, Devi S (2007) Synthesis of Au, Ag and Au–Ag alloy nanoparticles in aqueous polymer solution. Colloids Surf A Physicochem Eng Asp 302:51–57. https://doi.org/10.1016/j.colsurfa.2007.01.054

Publisher's Note